Proceedings of the 2nd ITB Graduate School Conference

Strengthening Multidisciplinary Research to Enhance its Impact on Society
July 21, 2022

Effect of Flexible Joint and Rigid Segment Variation on Soft Robotic Finger Kinematics

Akmal Reza Ahkam¹, Sandro Mihradi^{2*}, Vani Virdyawan³, F. Ferryanto² & Andi Isra Mahyuddin²

¹Graduate Student, Mechanical Engineering Study Program, Faculty of Mechanical and Aerospace Engineering, Institut Teknologi Bandung, Bandung, West Java, Indonesia

²Mechanical Design Research Group, Faculty of Mechanical and Aerospace Engineering, Institut Teknologi Bandung, Bandung, West Java, Indonesia

³Mechanical Production Engineering Research Group, Faculty of Mechanical and Aerospace Engineering, Institut Teknologi Bandung, Bandung, West Java, Indonesia.

*Email: sandro@ftmd.itb.ac.id

Abstract. The latest development in the robotic hand is the application of highly deformable materials for a hand structure known as a soft robotic hand. Soft robots have many advantages over conventional rigid bionic hands due to their lightweight and compliant characteristics. Although there are various designs of a soft robotic hand that could produce compliance mechanisms, one design that resembles a human finger's structure is a manipulator that uses flexible joints and rigid segments. The combination of these two elements would affect the finger's bending angle and motion range. This article reports the design and parametric study of the manipulator, which has four main components: silicone rubber, strain limiting layer, fiber reinforcements, and 3D print structures from polylactic acid (PLA). In addition, we deliver the optimum design manipulator model, which will be manufactured in the subsequent research.

Keywords: robotic hand; soft robot; finger; manipulator; parametric study; flexible joint; rigid segment.

1 Introduction

Robotic hands have expanded and have been utilized in various sectors. In the medical field, robotic hands substitute the amputated hand due to an accident or congenital disability. This robot is usually called a prosthetic hand/bionic hand [1]. Commercial Bionic hands (the i-Limb¹, the Bebionic², and the Michelangelo³) have robust mechanisms to accomplish hand functions with the EMG sensor, which is mounted onto the skin of the residual limb. Regardless of

ISSN: 2963-718X

¹ http://www.touchbionics.com

² http://www.bebionic.com

³ http://www.living-with-michelangelo.com/home

their satisfactory ability, the products are quite heavy (> 420 g) [1] and expensive (>US\$10,000) [2]. Soft robots are emerging and rapidly growing to handle established robots issue constructed by unbending structures [3]. These new robots are interesting because they could easily deform while being resilient, adapt to the surroundings without harming humans, and allow low-cost production [4]. Furthermore, elastic components could decrease the robot's weight.

An anthropomorphic hand design based on soft robotics technology could achieve dexterous grasping capabilities [5]. 1-chamber tube manipulator with a tapering shape at the tip and a thread winding is used on the robot, which weighs 178 g. However, the entire manipulator structure is fully elastic, unlike human fingers, which have rigid-bone anatomy. In one study, the manipulator is attached with plastic lamination as a rigid structure to mimic the human finger [2]. The addition of this rigid structure increases grip strength because of the wider manipulator's outer surface contact with the gripping object. Inspired by this configuration, we designed a finger manipulator with flexible joints and rigid segments.

The finite element analysis with Abaqus was conducted to optimize the kinematics of the soft robot finger. The simulation provides an effective solution to vary the component dimension and predict the performance of the model without manufacturing the robots, which could take a considerable amount of time. Finally, by the parameterization of wall thickness, fiber angle, fabric width, elastic section, and rigid section length, we could find the optimized design of soft manipulator from this method [6].

In this article, we start off with conceptual design of the model and conduct a finite element modelling. After that, the design variables are analyzed to understand their effect to the manipulator. The last is the simulation result and kinematics performance explanation about the robot.

2 Conceptual Design

Chamber design is an essential feature in which, upon pressurization, the air/fluid would press in all directions of the inner chamber wall and deform the manipulator. Although forming a multi-chambered manipulator could be made to control the manipulator's bending in a particular desired direction [7], the finger robot only requires the actuator to turn in one direction. Therefore, it does not need more than one chamber. There are three types of the manipulator [6]. The first type is the corrugated membrane which has a folds/fins on the actuator that expand under the pressure to make a bending motion. The second is the eccentric void asymmetries leading to different layer thicknesses in the actuator. And the

third is the multi-material types that is assembled from a combination of elastomeric and inextensible materials. This type possesses simpler tubular geometry that offers ease of manufacture [8]. In addition, we provided a fiber-reinforcement to avoid the radial expansion for optimizing the bending motion [9].

A design model arranged by two flexible joints and three rigid segments is manufactured and experimented with to prove the conceptual design. The casting process uses 3D printed molding (Figure 1a). The rigid structure from PLA is partially attached to the manipulator, fabric as a strain limiting layer is embedded into it, and fiber is wound along it (Figure 1b). A proof-of-concept prototype was then manufactured (see Figure 1c). During pressurization, the prototype achieved an appropriate bending movement, which demonstrates the feasibility of this design. Then, the finite element simulation is conducted to mimic the experiment (Figure 1d). From this early result, it is found that the specimen produced larger bending angle in the experiment than in the simulation.

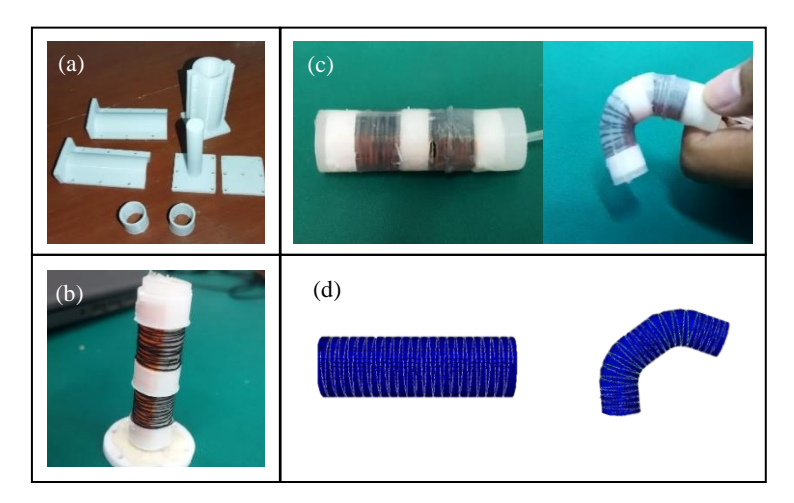


Figure 1 Manufacture, experiment, and finite element model of conceptual design approval. (a) 3D printed molding. (b) Manipulator model that has been attached by fabric layer, fiber winding, and rigid structure. (c) A proof-of-concept prototype. (d) Finite element simulation.

3 Finite Element Modelling

At the beginning stage of simulation, five variables were defined as independent variables, i.e. cylinder wall thickness, fiber winding angle, fabric width, elastic section length, and rigid section length. Then, the material properties of each component were explained to show the specific data that are utilized in the

simulation. The last stages were meshing, defining constraints, loads, and boundary conditions.

The finger manipulator model is presented in Figure 2. The main form of the manipulator is a single tubular and semicircular adjustment on the fingertip. The finger's length and diameter dimensions were adapted to the Indonesian's anthropometry [10]. Then, the fiber loops and a strain limiting layer were implanted and were simulated to achieve the optimal design.

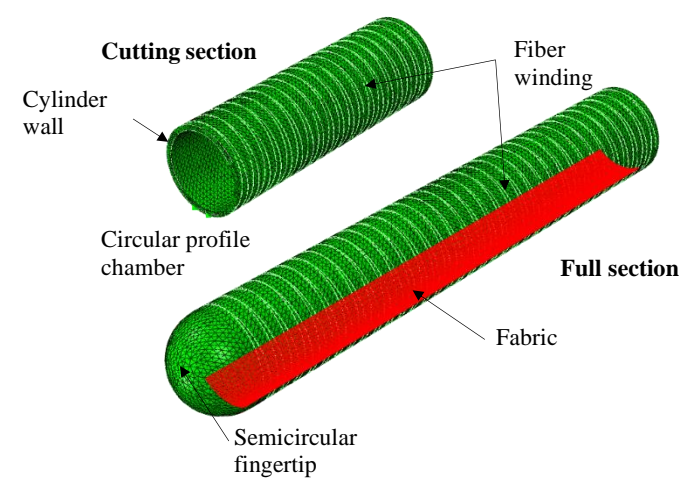


Figure 2 Full and cutting section of manipulator design.

3.1 Material Properties

In the simulation, the materials were determined based on secondary data [6]. The main part of the manipulator used one of the most widely used silicone rubbers, i.e., Ecoflex 30. The silicone will be partially wrapped using polylactic acid (PLA) as a rigid structure that resembles a finger segment. Ecoflex and PLA are the solid features that use Yeoh and Elastic model respectively. Then two fiber windings that used Kevlar material as beam feature were assigned with Elastic model, and the fabric used elastic material with Neo Hooke model and modifications to simulate a strain limiting layer that could withstand tensile loads but not bending loads. The detailed data applied in the simulation is shown in Table 1.

 Table 1
 Material properties and section assignments.

Material	Model	Coefficients	Section	
Ecoflex 30	Yeoh	$C_{10} = 0.11 MPa, C_{20} = 0.02 MPa$	Solid, type: Homogeneous	

PLA	Elastic	$E = 3000 MPa, \nu = 0.3$	Solid, type: Homogeneous
Kevlar	Elastic	E = 31067 MPa, v = 0.36	Beam, type: Constant
Fabric	Neo Hooke	$C_{10} = 100 Mpa$	Shell, type: Homogeneous

3.2 Meshing and Constrain

Ecoflex and PLA materials are the main construction of the manipulator modelled component. These two components are applied to tetrahedron mesh which is formulated in hybrid and quadratic geometric order because of the complex geometry. In Kevlar, the order linear geometric is utilized with a global meshing size of 0.3. This size is smaller than the Ecoflex/PLA meshing because Kevlar will be tied with the manipulator as the master surface. Fabric as an embedded region on the manipulator wall uses quad-dominated mesh control with a reduced integration method. A summary of the meshing process is presented in the following table.

MaterialMesh ControlElement Type CodeGlobal Size (mm)Ecoflex 30TetrahedronC3D10H1PLATetrahedronC3D10H1Kevlar-B310.3

0.5

Table 2 Meshing properties in each component.

The constraint between the inner and outer wall of the manipulator is defined as self-contact with 0.3 frictional force coefficient. If no constraint is specified, the simulation will stop at low pressure due to a lack of definition.

S4R

3.3 Boundary Condition and Load

Quad-dominated

Boundary conditions are placed at the base point of the manipulator finger, which has a circular surface with a fixed end so that the manipulator does not translate and rotate in that point. At the same time, the pressure load is given gradually from 0 to 1 MPa with 0.1-second increments, which exceeds the model's capability. Therefore, the simulation will abort when the manipulator has reached the maximum load.

4 Parametric Study

Fabric

Modeling is accomplished in two processes and gradually from one design variable to another. First, the model is fully elastic, varying the wall, fibers, and fabric layer. This modeling obtains the optimal model design that performs bending. Second, the simulation is carried out by varying the length of the elastic and rigid sections for kinematics analysis.

4.1 Wall Thickness, Fiber Angle, Layer Width

Figure 3 shows a visual illustration of the modeling carried out. In Model 1, the manipulator wall thickness is varied (1-3 mm) to observe the changes. With the same pressure input, the thicker wall has a small deformation but does not affect the fingertip trajectory. This wall thickness will affect how much pressure the manipulator can withstand and will be directly proportional to the compressive force that will be applied when later used to grip objects. Model 2 is a model with variations in the angle (3-15 degree) of the fiber winding. It could be seen that the tight winding of the fiber will resist the deformation in the radial direction so that the strain will be focused on the bending motion.

The parametric method used in Model 3 is the variation of the width of the strain limiting layer (12-60 mm). The wider the layer, the higher the stiffness of the manipulator because the elastic part is covered, so it cannot be deformed. However, if the fabric width is too small, the manipulator could bend out of the axis.

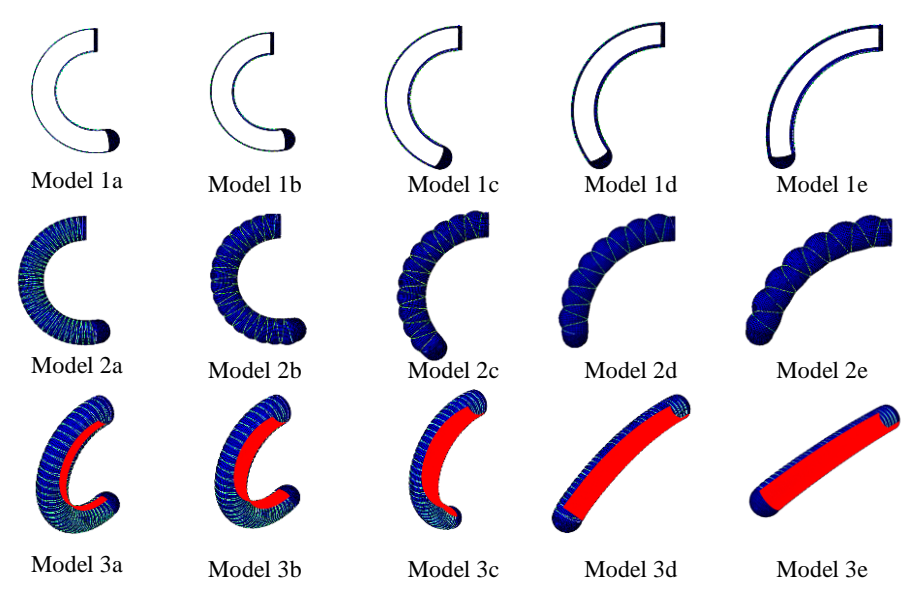


Figure 3 Finite element results for varying wall thickness, fiber angle, and fabric width.

4.2 Flexible Joint and Rigid Segment

Two critical elements, flexible joint and rigid segment, are rarely analyzed for how they affect the movement of the manipulator. Three independent variables L_M , L_P , and L_D are varied. The subscripts marked the length of the metacarpophalangeal, proximal interphalangeal, and distal interphalangeal. By obtaining the proportion of each length variable from the previous experiment [2], this variable is increased periodically by the initial length. This flexible joint difference will cause the dependent variable of the angle at the joints α_1 , α_2 and α_3 to change. The capital letters MCP (metacarpophalangeal), PIP (proximal interphalangeal), and DIP (distal interphalangeal) are indicating the location of the finger joints.

After obtaining the optimum length of the manipulator model, the length of the rigid segment was varied without changing the length of the flexible joint. This rigid segment variable is defined as R_1 , R_2 , and R_3 . The variable definition can be seen in Figure 4.

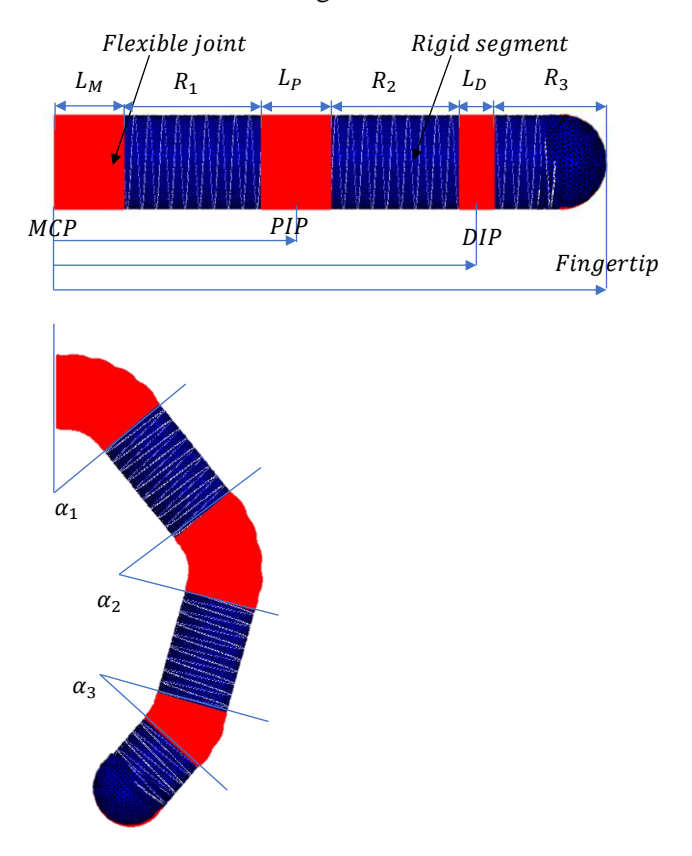


Figure 4 Variable design determination.

Visually, the simulation results can be seen in Figure 5. Model 4 is a design with variations in the length of the elastic section. While model 5 is a variation of rigid parts. Detailed data for each simulation will be presented in the next paragraph.

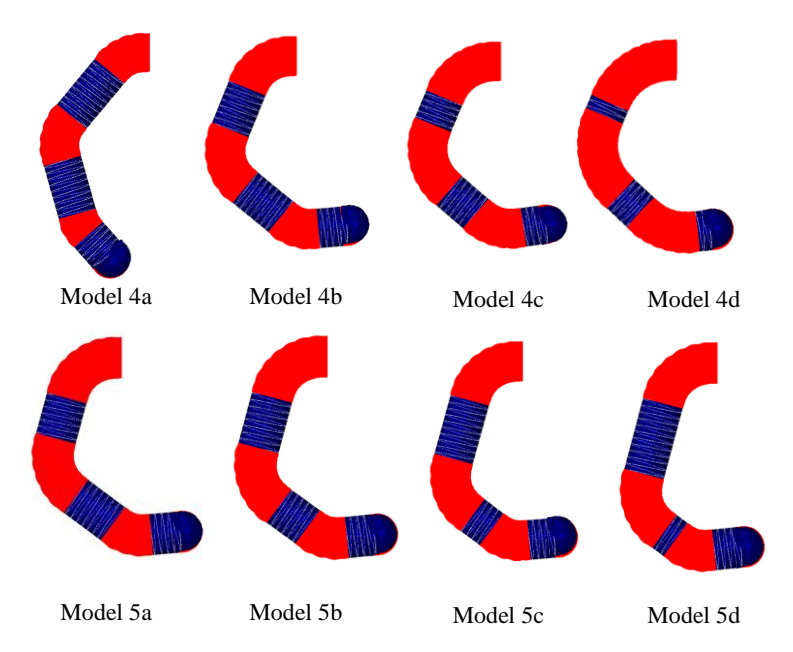


Figure 5 Visual illustration of flexible and rigid section modelling.

The elastic section simulation data can be seen in Table 3. The variation of elastic length is available along with the angle and maximum pressure that can be simulated. It could be seen that the longer the elastic section, the lower the pressure when the simulation stopped. There are two possibilities for this phenomenon, the material could no longer be deformed, or the material has failed. The assumption is supported by the total bending angle data, which can be seen in the a-total column. The simulation stops at a relatively close total angle in models 4b, 4c, and 4d. Model 4b was chosen as the optimal model based on the data and visual results from this modeling.

 Table 3
 Flexible joint model data.

Model	L_M (mm)	L_{P} (mm)	L_D (mm)	α ₁ (°)	α ₂ (°)	α ₃ (°)	α_{total} (°)	P_{max} (kPa)
4a	15	15	7.5	50.1	55.4	25.8	131.3	158
4b	20	20	12.5	66.9	71.8	43.6	182.3	150
4c	25	25	17.5	67.5	71.7	49.3	188.6	112
4d	30	30	22.5	66.6	70.2	49.6	186.4	90

From the flexible length section that has been obtained from the previous modeling, the variation data on the rigid section can be seen in Table 4. The variation is carried out on the variables R_1 and R_2 , where R_3 is a controlled constant. This simulation found that the length change in this rigid structure does not significantly affect the total angle of indentation. However, the difference is only seen in Model 5a, at angles α_2 and α_3 . So, the model selection is based on the location of the rigid structure close to finger joint anthropometry, which is Model 5b.

 P_{max} R_1 R_2 α_{total} Model (mm) (mm) (mm) (kPa)5a 20 25 19.5 74.9 41.9 68.9 185.8 142 5b 25 20 19.5 74.4 68.6 41.6 184.6 141 30 19.5 74.9 142 5c 15 68.7 41.9 185.6 35 5d 10 19.5 74.6 68.7 41.7 185.1 141

Table 4 Rigid segment model data.

5 Kinematics Performance

In this section, some of the kinematic performances of the optimum model that have been obtained are discussed. The bending angle at each joint is plotted and presented in Figure 6. It could be seen that the model maximum pressure could achieve 141 kPa. Moreover, the bending angle at the fingertip or α_{total} is 184.6 degrees, indicating that the finger manipulator could bend backward.

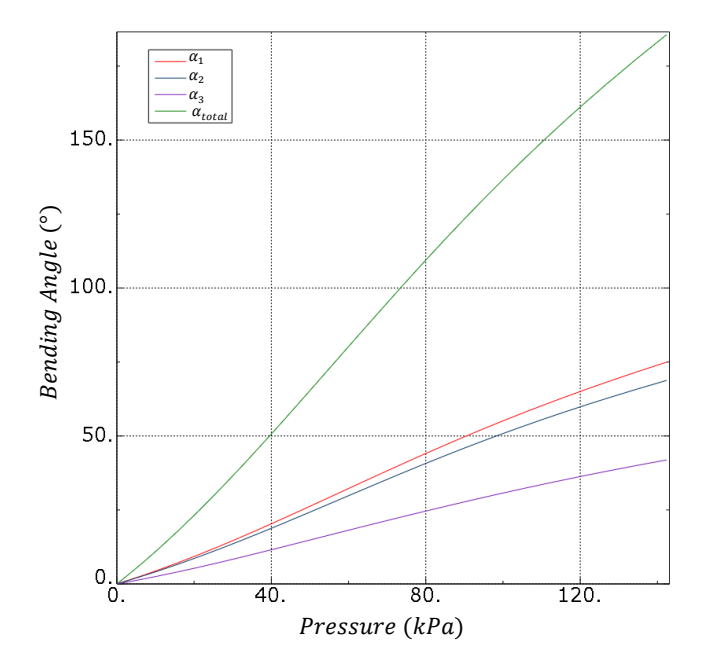


Figure 6 Bending angle of the manipulator.

The joints and fingertip movement of the manipulator are traced in the simulation. Then their line-trajectory model is illustrated in Figure 7. The curved line represents the manipulator finger motion range which assembles human finger kinematics [11]. This soft finger will be adaptive if there are objects that block the movement of the lower knuckles. Then the additional rigid structure of the finger will strengthen the manipulator.

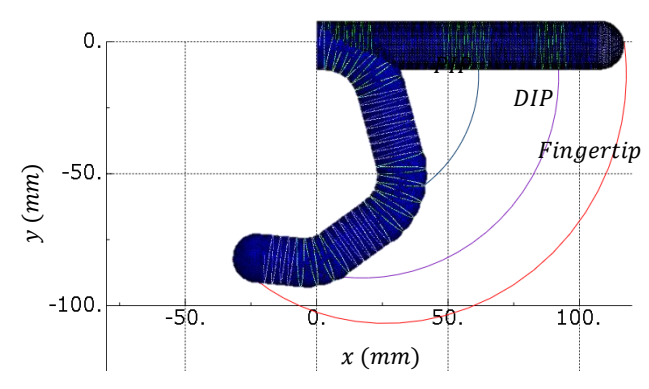


Figure 7 The line-trajectory model design of each joint.

6 Conclusion

A parametric study of the manipulator effect on each change in the design variable geometries is explained in this research. The design, which based on flexible joints and rigid segments are satisfying design that could mimic the kinematic performance of an adaptive human finger. It should be noted that the model of the strain limiting layer is still an assumption. Additionally, there is still a problem while performing the simulation at high pressures (e.g. more than 160 kPa). The validation of the simulation with experiments will be part of our future works. This research is the initial stage of making a soft robot hand. It is challenging to make a prototype of the finger and its mechanical and control system.

Funding

This work was supported by a Newton Fund Institutional Links grant, ID 623531377, under the Newton Fund Indonesia partnership. The grant is funded by the UK Department for Business, Energy and Industrial Strategy and Directorate of Resources Affairs Directorate General of Higher Education, Ministry of Education, Culture, Research and Technology, Republic of

Indonesia, contract no: 341/E4.1/AK.04.PT/2021 and delivered by the British Council.

References

- [1] F. Cordella *et al.*, "Literature review on needs of upper limb prosthesis users," *Front. Neurosci.*, vol. 10, no. MAY, 2016, doi: 10.3389/fnins.2016.00209.
- [2] G. Gu *et al.*, "A soft neuroprosthetic hand providing simultaneous myoelectric control and tactile feedback," *Nat. Biomed. Eng.*, 2021, doi: 10.1038/s41551-021-00767-0.
- [3] G. Bao *et al.*, "Soft robotics: Academic insights and perspectives through bibliometric analysis," *Soft Robot.*, vol. 5, no. 3, pp. 229–241, 2018, doi: 10.1089/soro.2017.0135.
- [4] N. El-Atab *et al.*, "Soft Actuators for Soft Robotic Applications: A Review," *Adv. Intell. Syst.*, vol. 2, no. 10, p. 2000128, 2020, doi: 10.1002/aisy.202000128.
- [5] R. Deimel and O. Brock, "A novel type of compliant and underactuated robotic hand for dexterous grasping," *Int. J. Rob. Res.*, vol. 35, no. 1–3, pp. 161–185, 2016, doi: 10.1177/0278364915592961.
- [6] M. S. Xavier, A. J. Fleming, and Y. K. Yong, "Finite Element Modeling of Soft Fluidic Actuators: Overview and Recent Developments," Adv. Intell. Syst., vol. 3, no. 2, p. 2000187, 2021, doi: 10.1002/aisy.202000187.
- [7] A. Garriga-Casanovas, I. Collison, and F. Y. Rodriguez Baena, "Toward a Common Framework for the Design of Soft Robotic Manipulators with Fluidic Actuation," *Soft Robot.*, vol. 5, no. 5, pp. 622–649, 2018, doi: 10.1089/soro.2017.0105.
- [8] P. Polygerinos *et al.*, "Modeling of Soft Fiber-Reinforced Bending Actuators," vol. 31, no. 3, pp. 778–789, 2015.
- [9] F. Connolly, C. J. Walsh, and K. Bertoldi, "Automatic design of fiber-reinforced soft actuators for trajectory matching," vol. 114, no. 1, pp. 51–56, 2017, doi: 10.1073/pnas.1615140114.
- [10] H. Purnomo, "PENGUKURAN ANTROPOMETRI TANGAN USIA 18 SAMPAI 22 TAHUN KABUPATEN SLEMAN YOGYAKARTA Hari Purnomo Jurusan Teknik Industri, Fakultas Teknologi Industri Universitas Islam Indonesia," *Semin. Nas. Ind. Eng. Natl. Conf.*, no. 2004, pp. 106–112, 2014.
- [11] J. Won and N. Robson, "Control-Oriented Finger Kinematic Model: Geometry- Based Approach," vol. 11, no. December, pp. 1–10, 2019, doi: 10.1115/1.4044601.